

Global study of quadrupole correlation effect

Yi Li (李义)

School of Physics and Astronomy, Sun Yat-Sen University

Journal Club (20250416)

Reference: M. Bender, G. F. Bertsch, and P.-H. Heenen, Global study of quadrupole correlation effects, PRC 73, 034322 (2006)

Global study of quadrupole correlation effects

M. Bender,^{1,2,3} G. F. Bertsch,¹ and P.-H. Heenen⁴

¹*Department of Physics and Institute for Nuclear Theory, Box 351560, University of Washington, Seattle, Washington 98195, USA*

²*Physics Division, Argonne National Laboratory, 9700 S. Cass Avenue, Argonne, Illinois 60439, USA*

³*National Superconducting Cyclotron Laboratory, Michigan State University, East Lansing, Michigan 48824, USA*

⁴*Service de Physique Nucléaire Théorique, Université Libre de Bruxelles, CP 229, B-1050 Brussels, Belgium*

(Received 26 August 2005; published 29 March 2006)

We discuss the systematics of ground-state quadrupole correlations of binding energies and mean-square charge radii for all even-even nuclei, from ^{16}O up to the superheavies, for which data are available. To that aim we calculate their correlated $J = 0$ ground state by means of the angular-momentum and particle-number projected generator coordinate method, using the axial mass quadrupole moment as the generator coordinate and self-consistent mean-field states restricted only by axial, parity, and time-reversal symmetries. The calculation is performed within the framework of a nonrelativistic self-consistent mean-field model by use of the same Skyrme interaction SLy4 and to a density-dependent pairing force to generate the mean-field configurations and to mix them. These are the main conclusions of our study: (i) The quadrupole correlation energy varies between a few 100 keV and about 5.5 MeV. It is affected by shell closures, but varies only slightly with mass and asymmetry. (ii) Projection on angular momentum $J = 0$ provides the major part of the energy gain of up to about 4 MeV; all nuclei in the study, including doubly magic ones, gain energy by deformation. (iii) The mixing of projected states with different intrinsic axial deformations adds a few 100 keV up to 1.5 MeV to the correlation energy. (iv) Typically nuclei below mass $A \leq 60$ have a larger correlation energy than static deformation energy whereas the heavier deformed nuclei have larger static deformation energy than correlation energy. (v) Inclusion of the quadrupole correlation energy improves the description of mass systematics, particularly around shell closures, and of differential quantities, namely two-nucleon separation energies and two-nucleon gaps. The correlation energy provides an explanation of “mutually enhanced magicity.” (vi) The correlation energy tends to decrease the shell effect on binding energies around magic numbers, but the magnitude of the suppression is not large enough to explain the relative overbinding at $N = 82$ and $N = 126$ neutron-shell closures in mean-field models. (vii) Charge radii are also found to be sensitive to the quadrupole correlations. Static quadrupole deformations lead to a significant improvement of the overall systematics of charge radii. The dynamical correlations improve the local systematics of radii, in particular around shell closures. Although the dynamical correlations might reduce the charge radii for specific nuclei, they lead to an overall increase of radii when included, in particular in light nuclei.

- Considering phenomenological corrections, the self-consistent mean-field (SCMF) theory yields a mass prediction accuracy with a rms deviation of about **0.6–0.7 MeV**, which is far less accurate than that of local mass models (rms ~ **100 keV**).

“not a physical phenomenon, but rather a characteristic arising from the mean-field approximation”

- Stripping away all phenomenological corrections, the SCMF theory yields a rms deviation in the range **1.5-1.7 MeV**.

We need to treat the correlations explicitly!

- The mean-field approach works well for the short-range character of the nucleon-nucleon interaction. However, long-range correlations come about when a symmetry is broken.
- There are two way to consider long-range correlations effects: (Q)RPA, GCM

(Q)RPA

- (i) The RPA does not converge well when the interactions are short ranged [15]. This becomes obvious when one notes that second-order perturbation theory for a contact interaction diverges and that the usual formula for the RPA correlation energy incorporates the second-order perturbation.
- (ii) As a small-amplitude approximation, the QRPA cannot be expected to give a good description of the correlated ground-state wave function in soft transitional nuclei and nuclei with coexisting minima, where the ground-state is spread over a wide range of deformations.

GCM ✓

- (i) Convergence can be an issue on a numerical level. The theory is usually couched in terms of a continuum of mean-field states, but in practice computations are carried out with finite sets of states. If there are too many states in the basis of nonorthogonal states, they will be redundant and the matrix techniques to find the lowest-energy state become unstable.
- (ii) For numerical reasons, we are limited at present to a single external field. We take it to be the isoscalar axial quadrupole field,

$$Q_2 = 2z^2 - x^2 - y^2, \quad (1)$$

leaving out higher multipoles and nonaxial quadrupolar deformations.

- (iii) Already for $J = 2$ excitations, it may be insufficient to take only the single generating field from Eq. (1). This suspicion is raised by systematic overestimations of quadrupole excitations in rigid spherical nuclei [19,20].

In this paper we aim at a systematic study of the quadrupole correlation energy for all even-even nuclei for which the mass is known.

➤ Mean field

- Nonrelativistic Skyrme interaction SLy4 with pairing effects which treated in the BCS approximation by use of a density dependent zero-range force.
- Self-consistent mean-field states are restricted only by axial, parity, and time-reversal symmetries.
- The SCMF states $|q\rangle$ are constrained to different quadrupole moments

$$q = \langle Q_2 \rangle$$

where $Q_2 = 2z^2 - x^2 - y^2$. Higher even axial multipole moments are automatically optimized for a given mass quadrupole moment.

$$\beta_2 = \sqrt{\frac{5}{16\pi} \frac{4\pi}{3R^2A}} \langle \hat{Q}_2 \rangle$$

- Single-particle wave functions are discretized on a three-dimensional Lagrange mesh corresponding to a cubic box.

➤ Beyond the Mean Field

- The mixed projected many-body state (or GCM) state is set up as a coherent superposition of normalized projected mean-field states $|JMq\rangle$ with different intrinsic deformations q

$$|J Mk\rangle = \sum_q f_{Jk}(q) |JMq\rangle$$

where $|JMq\rangle = \hat{P}_{MK} \hat{P}_N \hat{P}_Z |q\rangle$.

$$\hat{P}_N(N_0) = \frac{1}{\pi} \int_0^\pi d\phi_N e^{i\phi_N(\hat{N}-N_0)}, \quad \hat{P}_{MK}^J = \frac{2J+1}{16\pi^2} \int_0^{4\pi} d\alpha \int_0^\pi d\theta \sin(\theta) \int_0^{2\pi} d\gamma \mathcal{D}_{MK}^{*J} \hat{R},$$

- The f_{Jk} are given by solving the Hill-Wheeler-Griffin (HWG) equation

$$\sum_{q'} [H_J(q, q') - E_k I_J(q, q')] f_{Jk}(q') = 0$$

where the norm and Hamiltonian kernels are given by

$$I_J(q, q') = \langle JMq | JMq' \rangle = \frac{1}{N_J(q) N_J(q')} \int_0^{\pi/2} d\theta \sin(\theta) d_{00}^J(\theta) \langle q | \hat{R}(\theta) | q' \rangle$$

$$H_J(q, q') = \langle JMq | \hat{H} | JMq' \rangle = \frac{1}{N_J(q) N_J(q')} \times \int_0^{\pi/2} d\theta \sin(\theta) d_{00}^J(\theta) \langle q | \hat{R}(\theta) \hat{H} | q' \rangle$$

$$N_J(q) = \sqrt{\int_0^{\pi/2} d\theta \sin(\theta) d_{00}^J(\theta) \langle q | \hat{R}(\theta) | q \rangle}$$

➤ Beyond the Mean Field

- The mixed projected many-body state (or GCM) state is set up as a coherent superposition of normalized projected mean-field states $|JMq\rangle$ with different intrinsic deformations q

$$|J Mk\rangle = \sum_q f_{Jk}(q) |JMq\rangle$$

where $|JMq\rangle = \hat{P}_{MK} \hat{P}_N \hat{P}_Z |q\rangle$.

$$\hat{P}_N(N_0) = \frac{1}{\pi} \int_0^\pi d\phi_N e^{i\phi_N(\hat{N}-N_0)}, \quad \hat{P}_{MK}^J = \frac{2J+1}{16\pi^2} \int_0^{4\pi} d\alpha \int_0^\pi d\theta \sin(\theta) \int_0^{2\pi} d\gamma \mathcal{D}_{MK}^{*J} \hat{R},$$

- The f_{Jk} are given by solving the Hill-Wheeler-Griffin (HWG) equation

$$\sum_{q'} [H_J(q, q') - E_k I_J(q, q')] f_{Jk}(q') = 0$$

where the norm and Hamiltonian kernels are given by

$$I_J(q, q') = \langle JMq | JMq' \rangle = \frac{1}{N_J(q) N_J(q')} \int_0^{\pi/2} d\theta \sin(\theta) d_{00}^J(\theta) \langle q | \hat{R}(\theta) | q' \rangle$$

$$H_J(q, q') = \langle JMq | \hat{H} | JMq' \rangle = \frac{1}{N_J(q) N_J(q')} \times \int_0^{\pi/2} d\theta \sin(\theta) d_{00}^J(\theta) \langle q | \hat{R}(\theta) \hat{H} | q' \rangle$$

Reduce the number of
kernels that need to be
calculated exactly.

$$N_J(q) = \sqrt{\int_0^{\pi/2} d\theta \sin(\theta) d_{00}^J(\theta) \langle q | \hat{R}(\theta) | q \rangle}$$

Reduce the
number of
discrete θ

An approximation to the norm and Hamiltonian kernels as a function of θ is given by a two-point approximation

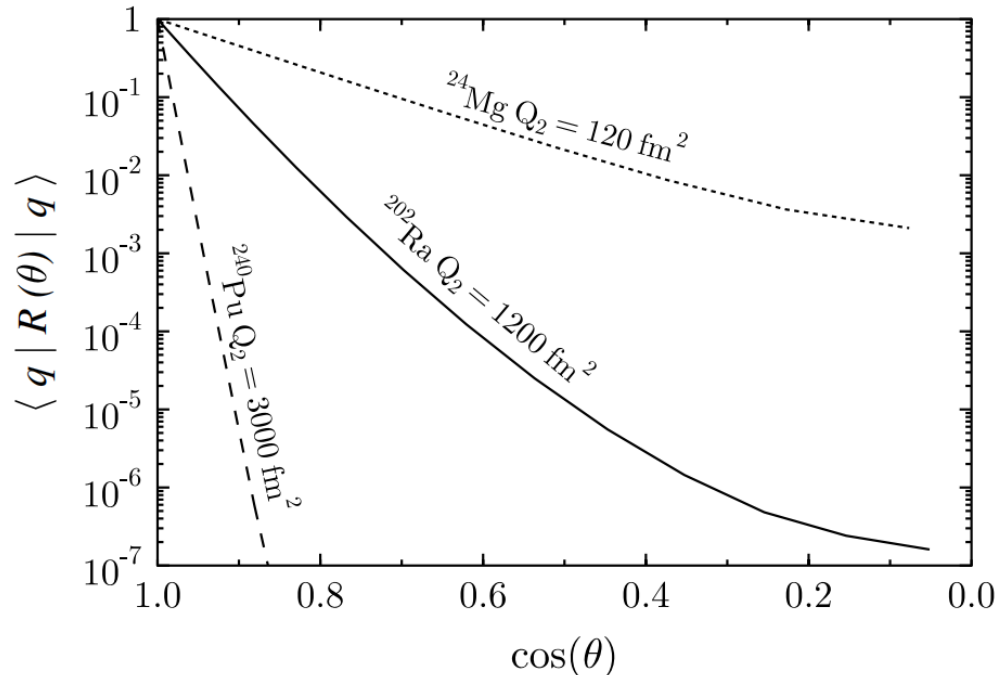
$$\langle q | \hat{R}(\theta) | q' \rangle = \langle q | q' \rangle e^{-c_2(q, q') \sin^2(\theta)}$$

$$\langle q | \hat{R}(\theta) \hat{H} | q' \rangle = \langle q | q' \rangle e^{-c_2(q, q') \sin^2(\theta)} [h_0(q, q') - h_2(q, q') \sin^2(\theta)]$$

where $\langle q | q' \rangle$ is the overlap between unrotated states, $h_0(q, q')$ is the Hamiltonian kernel between unrotated states.

The widths of the Gaussian and the expansion coefficient in the Hamiltonian kernel are determined by

$$c_2(q, q') = \langle q | \hat{R}(\theta_2) | q' \rangle, h_2(q, q') = \langle q | \hat{R}(\theta_2) \hat{H} | q' \rangle$$



- For magic nuclei and small deformations, the overlaps do not decrease strongly with θ_2 whereas for well-deformed ^{204}Pu , at the ground-state deformation, it falls by 2 orders of magnitude at a rotation angle of 15° .

- The angle θ_2 has to be chosen large enough to be sensitive to the variation of the overlap, but small enough to fit the integrand in the region to which it brings a large contribution.
- θ_2 is chosen to give an overlap of $1/2$

$$\langle q | \hat{R}(\theta) | q \rangle \approx \exp\{-[1 - \cos(\theta)]\langle \hat{J}_\perp^2 \rangle\}$$

and if the equation has no solution we set $\cos(\theta_2) = 1/\sqrt{2}$. For matrix elements between different states, $\langle \hat{J}_\perp^2 \rangle$ is chosen the larger one.

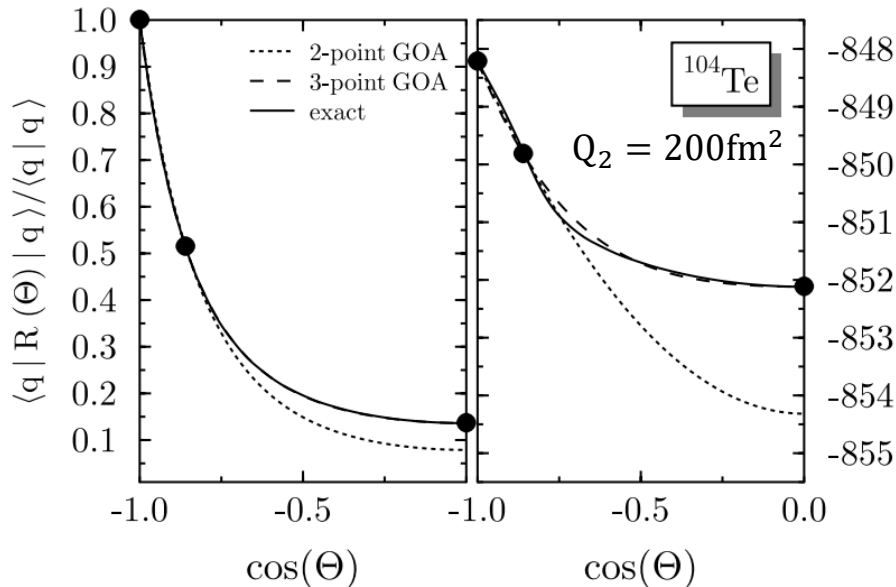
When the overlap varies slowly with the rotation angle we need three-point topGOA.

- nuclei with less than 22 neutrons or protons.
- configurations with very small prolate or oblate deformation.
- heavy nuclei differ from magic numbers by two nucleons or by an α particle.

$$\langle q | \hat{R}(\theta) | q' \rangle = \langle q | q' \rangle e^{-c_2(q, q') \sin^2(\theta) - c_4(q, q') \sin^4(\theta)}$$

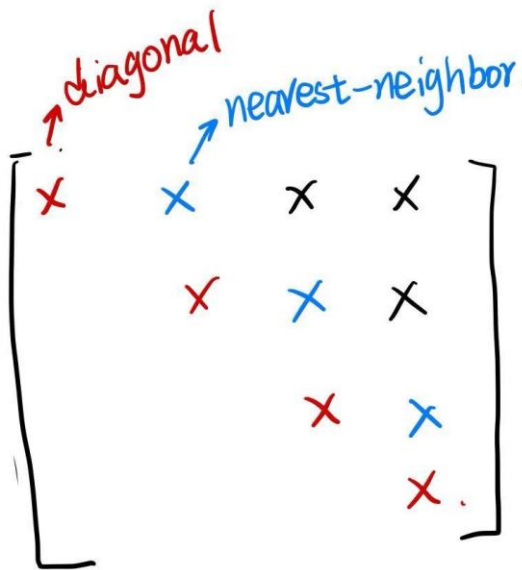
$$\begin{aligned} \langle q | \hat{R}(\theta) \hat{H} | q' \rangle &= \langle q | q' \rangle e^{-c_2(q, q') \sin^2(\theta) - c_4(q, q') \sin^4(\theta)} \\ &\times [h_0(q, q') - h_2(q, q') \sin^2(\theta) - h_4(q, q') \sin^4(\theta)] \end{aligned}$$

The additional parameter c_4 and h_4 are obtained by demanding exact values for the angles $\theta = 0, \theta_2$ and $\theta_3 = \pi/2$.



Method	$\langle q \hat{P}_{00}^0 q \rangle$	$\langle q \hat{P}_{00}^0 \hat{H} q \rangle / \langle q \hat{P}_{00}^0 q \rangle$
Two-point topGOA	0.0618	-850.753
Three-point topGOA	0.0705	-850.487
Full projection	0.0706	-850.488

- The configurations used for the GCM requires that the overlaps between neighboring configurations be above 0.5 and below 0.7.
- The calculation of overlap and Hamiltonian kernel need only diagonal and nearest-neighbor off-diagonal matrix elements



✓ $2n_c + 1$ elements per matrix

Mixing deformations



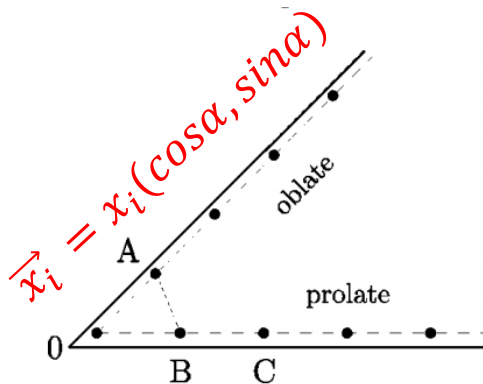
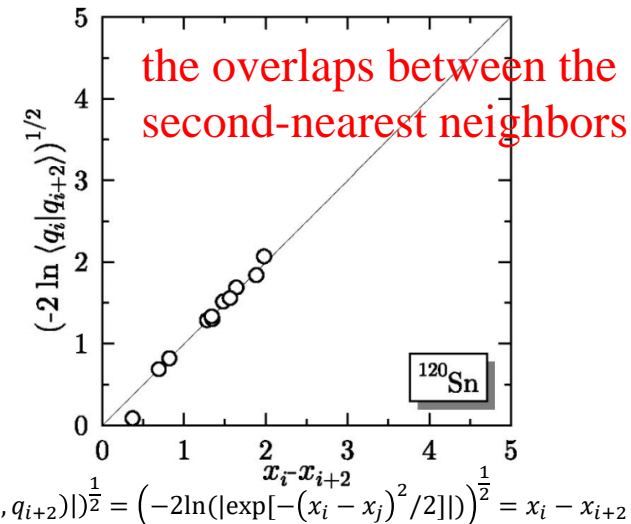
Other terms of $I_0(q_i, q_j)$ are approximated as

$$I_0(q_i, q_j) \approx \exp[-(x_i - x_j)^2/2]$$

where x_i is determined by

$$x_i = x_{i-1} + \sqrt{-2\ln[|I_0(q_i, q_{i+1})|]}$$

with (arbitrary) initial value $x_i = 0$.



$$\vec{x}_i = (x_i, 0)$$

$$\alpha = 30^\circ \sim 60^\circ$$

set as 45° in paper

Other terms of $H_0(q_i, q_j)$ are approximated as

$$H_0(q_i, q_j) = h(q_i, q_j)I_0(q_i, q_j)$$

$$h(q_i, q_j) = \frac{1}{2} [h(q_i, q_i) + h(q_j, q_j)] + \overline{h_2} |\vec{x}_i - \vec{x}_j|^2$$

where $\overline{h_2}$ is the average of all h_2

$$h_2(i, i+1) = \frac{1}{|\vec{x}_i - \vec{x}_{i+1}|^2} \left(\frac{h(q_i, q_i) + h(q_{i+1}, q_{i+1})}{2} - h(q_i, q_{i+1}) \right)$$

M. Bender, PRC 69, 034340, (2004)

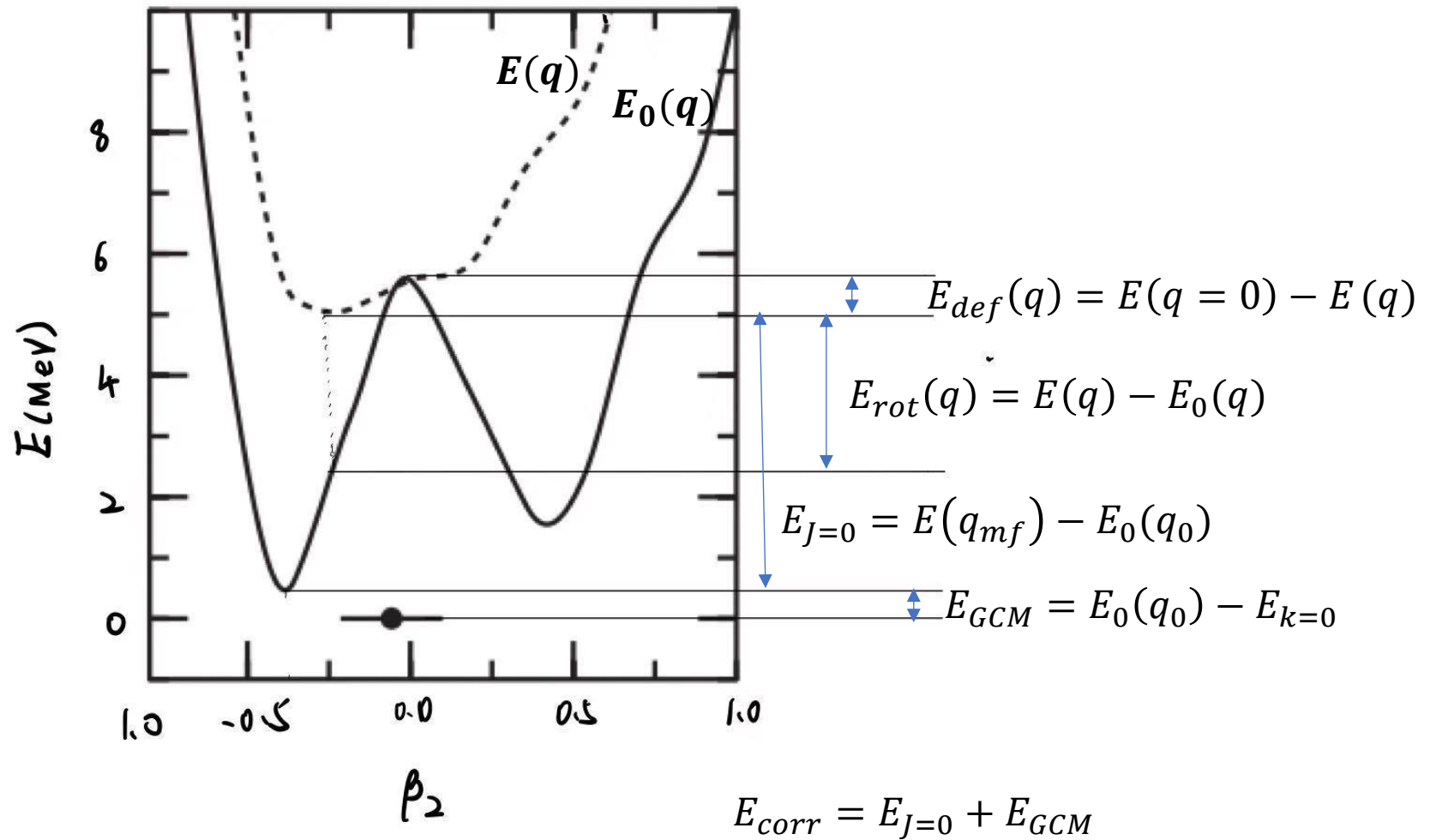
- ◆ Particle-number projection is still performed exactly.
- ◆ Projection on angular momentum requires n_j Euler angles (5–15) and the GCM mixing in quadrupole moment n_c deformed states (7–25).

$$n_j n_c (n_c + 1) / 2 \approx 150 - 5000$$

GOA saves a factor of 2 to 3 on n_j as well as a much larger factor on completing the GCM matrices.

$$n_j [n_c + (n_c - 1)] \approx 26 - 100$$

- ◆ The GOA is designed to describe accurately the correlations in the **0^+ ground state**.
- ◆ Achieving a total **accuracy of better than 300 keV**. This is sufficient for a study of the systematics of quadrupole correlation energies, which are an order of magnitude larger.



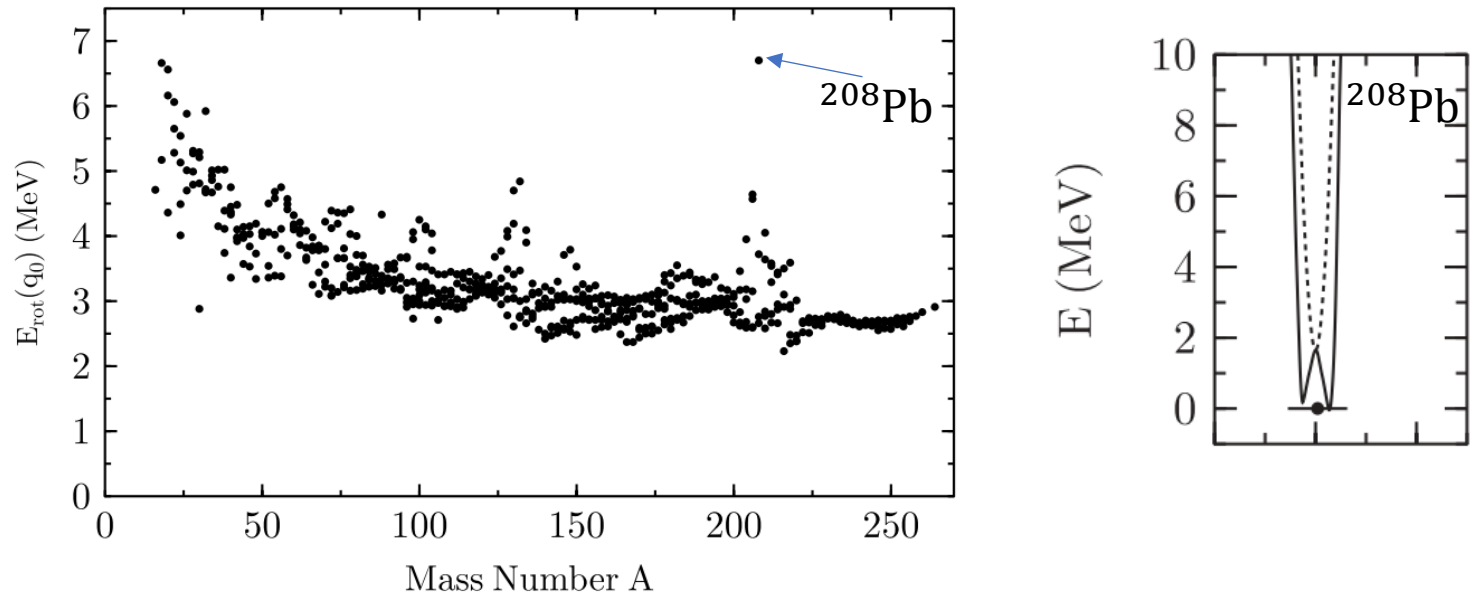
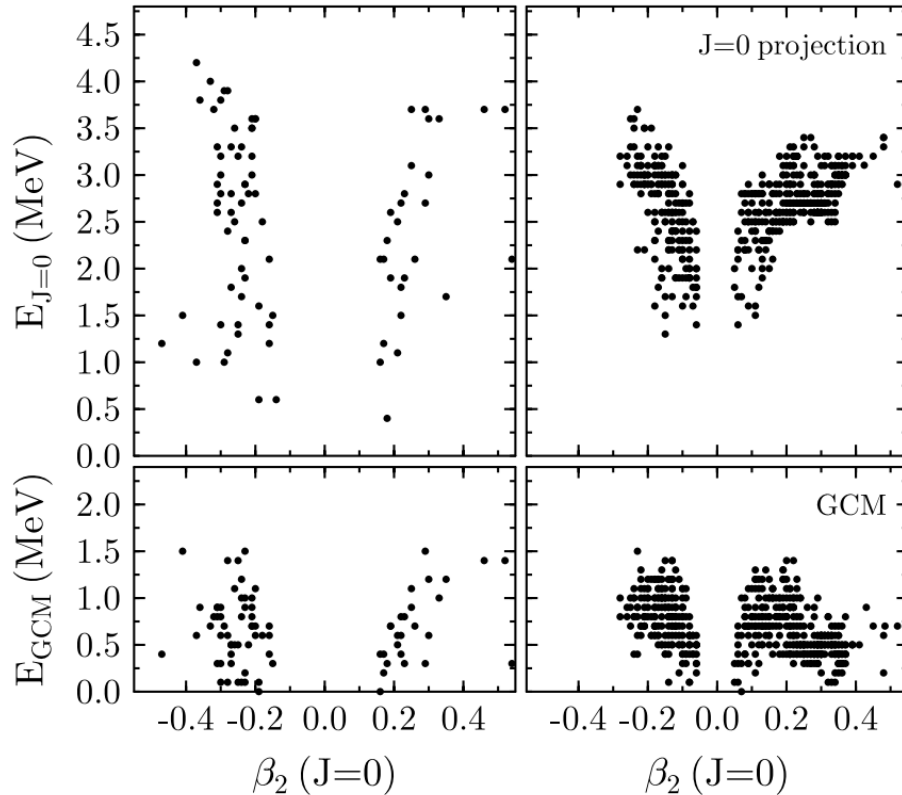


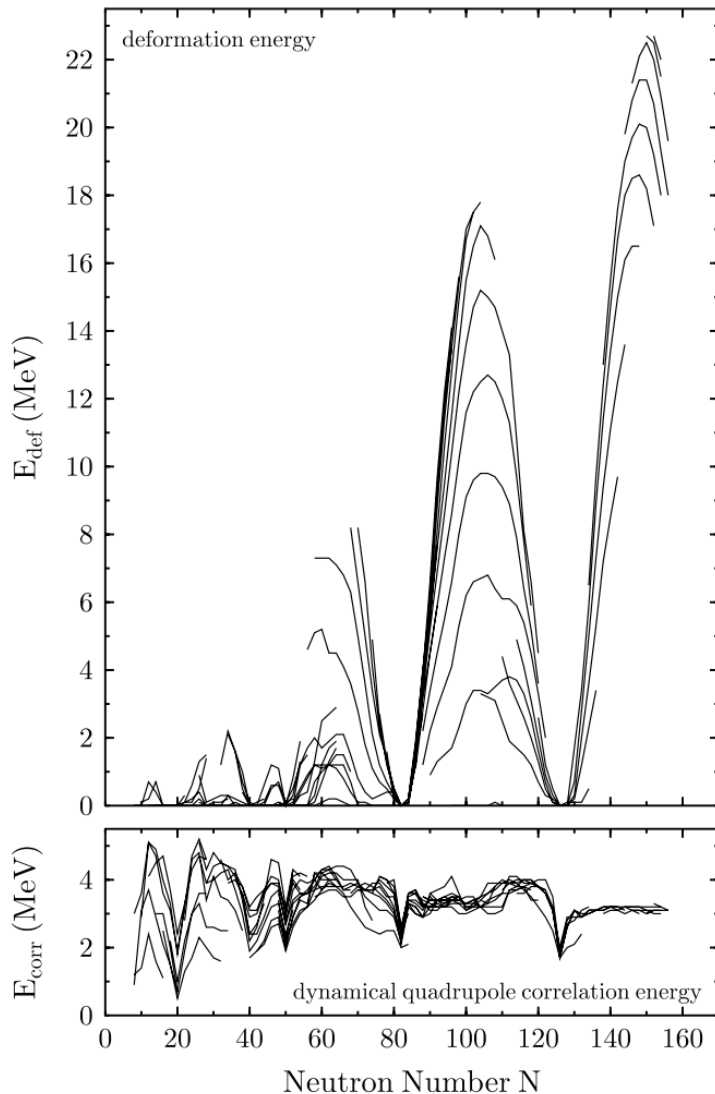
FIG. 5. Rotational energy $E_{\text{rot}}(q_0)$ at the minimum of the $J = 0$ projected energy curve.

- 605 nuclei that we have calculated.
- They vary rather smoothly, decreasing from about 6 MeV in light nuclei to 2.5 MeV for heavy ones.
- A few nuclei around the doubly magic ^{132}Sn and ^{208}Pb , $E_{\text{rot}}(q_0)$ is much larger and deviates from the general trend.

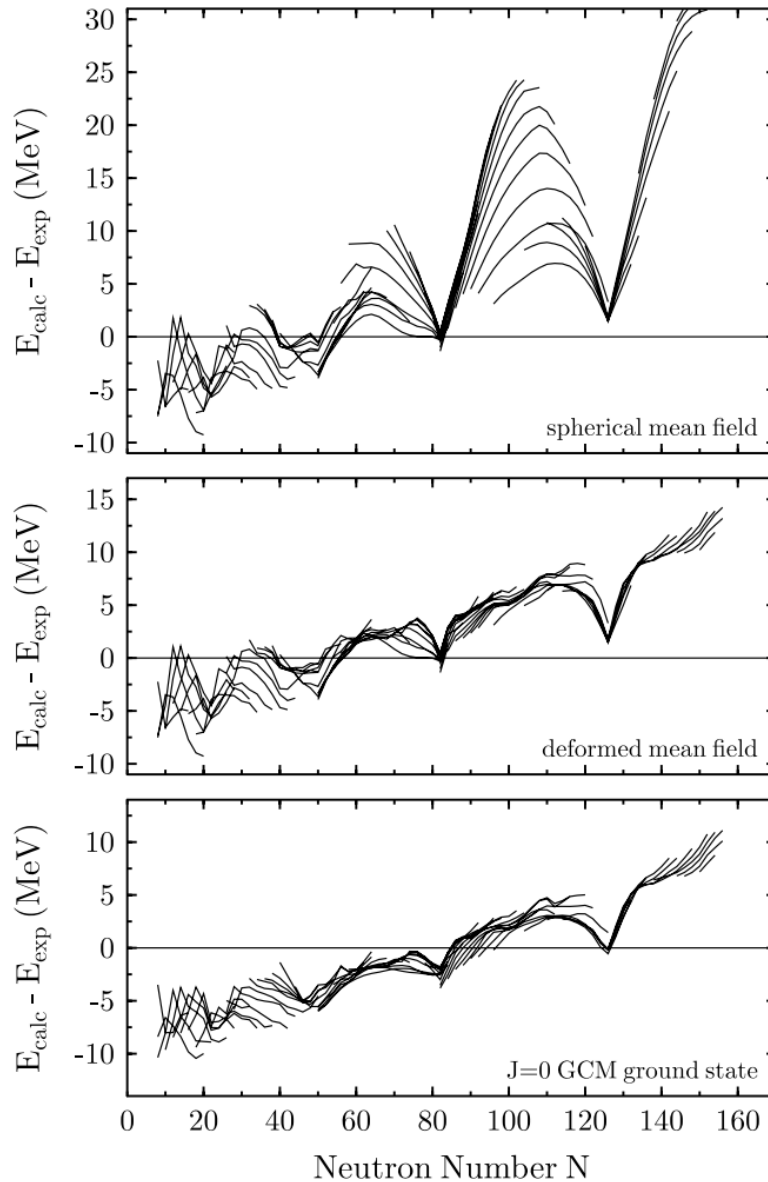


Left-hand and right-hand panels show light and heavy nuclei, respectively, divided at $A = 60$

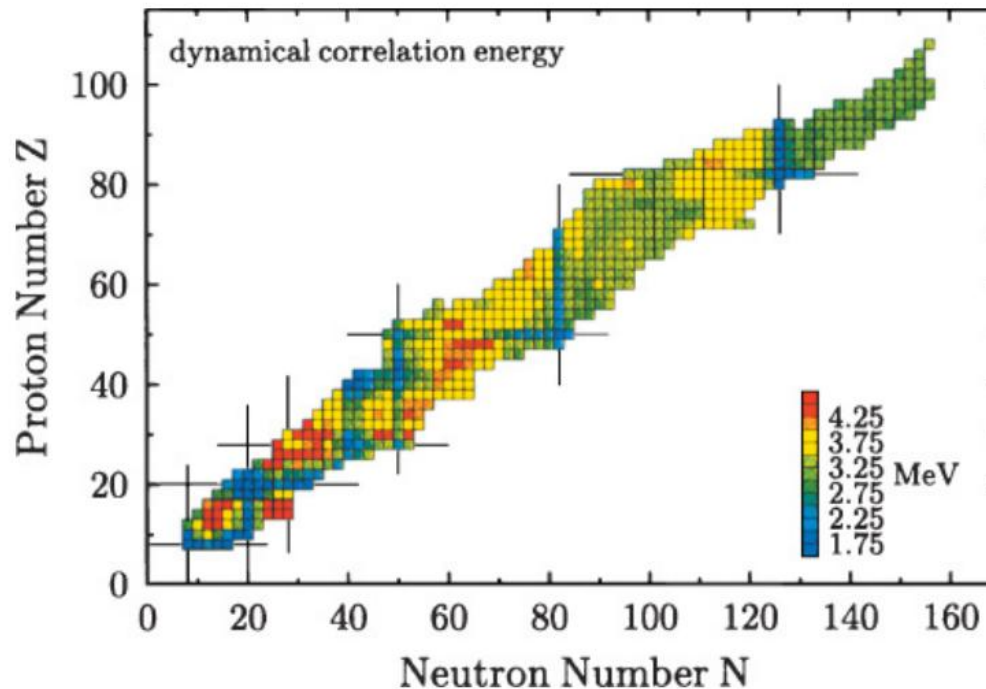
- Oblate and prolate configurations lead to correlation energies $E_J = 0$ of the same magnitude, with a large spreading as a function of β_2 , smaller for heavy nuclei than for light ones.
- For deformations larger than $\beta_2 = 0.2$, these energies vary for heavy nuclei between 2.5 and 3.5 MeV and for light ones between 1.0 and 4.2 MeV.
- E_{GCM} is small than $E_J = 0$ with a similar behavior for heavy and light nuclei.
- E_{GCM} ranges from 0 to 1.5 MeV and have no clear dependence on the sign or magnitude of β_2



- Both static and dynamic correlation energies are close to zero for doubly-magic nuclei.
- In light nuclei, the static correlation energy never exceeds a few MeV, whereas while it grows up to 18 MeV for A between 150 and 180.
- The dynamical correlation energy is close to 4 MeV for mid-shell nuclei and decreases slightly for heavy ones.



- Restricting the mean field to spherical shapes causes huge fluctuations of the mass residuals for heavy open-shell nuclei.
- For deformed mean field, the amplitude and spread of fluctuations decrease.
- Dynamical quadrupole correlations reduce the fluctuations by approximately a factor of 2.



- The smallest correlation energies are obtained for magic nuclei and the largest for transitional nuclei in the vicinity of shell closures.
- The correlation energy is nearly constant for rare-earth ($Z=57-71$) and actinide nuclei ($Z = 89-103$), which all have a static deformation.
- For neutron shell, the correlation energies are predicted to be very stable (besides $N=28$). For proton shells, the correlation energy is quite small around doubly magic nuclei, but rises substantially when one is going along the shell to mid neutron-shell nuclei.

TABLE V. Root-mean-square residuals of the binding energy and various binding-energy differences for spherical mean-field states, mean-field ground states, and the $J = 0$ projected GCM ground states ✓ as obtained with SLy4. All energies are in MeV.

Theory	E	S_{2n}	S_{2p}	δ_{2n}	δ_{2p}	Q_α
Spherical SCMF	11.7	1.6	1.6	1.2	1.1	2.1
Deformed SCMF	5.3	1.1	1.0	1.2	1.1	1.1
+ $J = 0$	4.4	0.9	0.8	0.9	1.0	0.9
+GCM	4.4	0.8	0.8	0.8	0.9	0.8

Since with SLy4 light nuclei are already predicted overbound by the mean-field ground state, correlations only worsen the situation. Therefore the correlations cannot improve the binding energy residuals.

two-nucleon separation energies

two-nucleon gaps

$$S_{2n}(N, Z) = E(N - 2, Z) - E(N, Z),$$

$$\delta_{2n}(N, Z) = E(N, Z - 2) - 2E(N, Z) + E(N, Z + 2)$$

$$S_{2p}(N, Z) = E(N, Z - 2) - E(N, Z).$$

$$\delta_{2p}(N, Z) = E(N - 2, Z) - 2E(N, Z) + E(N + 2, Z).$$

TABLE VI. The same as Table V, but for heavy nuclei with $N, Z > 30$ only.

Theory	E	S_{2n}	S_{2p}	δ_{2n}	δ_{2p}	Q_α
Spherical SCMF	12.6	1.6	1.5	0.9	0.6	2.1
Deformed SCMF	5.5	0.9	0.6	0.9	0.6	0.9
+ $J = 0$	3.9	0.8	0.5	0.7	0.5	0.8
+GCM	3.8	0.7	0.5	0.5	0.4	0.7

- Including quadrupolar correlations brings a large improvement; the correlation energies have the right qualitative behavior and also the right order of magnitude.
- With the original Skyrme interaction SLy4, the amplitude of the arches is decreased. The residuals of the masses still remain large, but in particular mass differences around magic numbers become rather accurate.
- Our aim here was to **determine the effect of correlations on residuals of binding energies** and to see whether they have the right tendencies to remove the deficiencies of pure mean-field calculations. **Our results for binding energies are encouraging in this respect.** Energy differences are less sensitive to wrong global trends of effective interactions, and the fact that they are significantly improved by correlations is a clear sign of **the necessity to go beyond the mean field.**